

Nonlinear Torque Control of the Induction Motor in Hybrid Electric Vehicle Applications

Sabri Dilmi
Teradyne Inc.

321 Harrison Av., Boston MA 02118
Email: dilmi.sabri@teradyne.com

Stephen Yurkovich

Center for Automotive Research
The Ohio State University
930 Kinear Rd, Columbus OH 43212
Email: yurkovich@ece.osu.edu

Abstract—In this paper, the torque tracking problem of the induction motor for Hybrid Electric Vehicle (HEV) applications is addressed. Because the standard Field Oriented Control (FOC) provides poor performance under rotor resistance uncertainty, a new robust controller-observer combination is designed in this paper in order to improve the overall performance. Our controller is based on a new PI-based extension of the FOC controller while our flux observer is based on the sliding mode technique. Simulation results show robustness with respect to rotor resistance uncertainty. A new optimal flux reference is derived to minimize the consumption of electrical energy, rather than the commonly used standard flux reference that maximizes motor torque. This choice is justified by the use of our controller in HEV applications. Simulation results show a significant reduction (35%) in energy losses.

I. INTRODUCTION

The automotive industry is increasingly seeking cleaner and more energy-efficient vehicles. The Hybrid Electric Vehicle (HEV) is one of solutions that assures lower gas emissions while saving energy usage. An HEV vehicle usually has two sources of traction; a combustion engine and an electric motor. The coupling of these two components can be in parallel or in series. In the parallel configuration, both the engine and the electric motor contribute to the traction force that moves the vehicle. Power is split between them according to a control strategy, which is usually implemented by a supervisory controller. Two different sub-controllers independently control the engine and the motor. Both sub-controllers receive their commands from the supervisory controller. Among these commands are the two torque requests required from both sub-systems as shown in Figure 1.

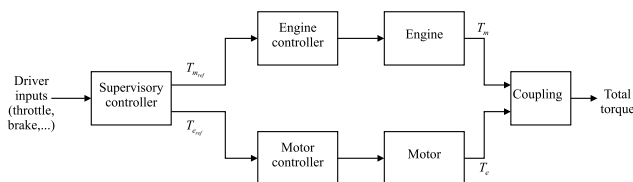


Fig. 1. Controllers hierarchy in a typical HEV application.

The induction motor is well suited for the HEV application because of its advantages over other types of

electric motors. For instance, it is more reliable due to the absence of brushes, it is more rugged due to its inherent one piece rotor shaft, it is safer when used in hazardous environments, and it presents a low cost solution. However, the development of a drive system based on the induction motor is not straightforward because of the complexity of the control problem involved with the induction motor. Early approaches were primarily based on the so-called scalar control techniques and were used only in constant speed applications. In the early 1970's Haase and Blaschke developed the new Field Orientated Controller (FOC) for a high performance induction motor drive system. This was based on rewriting the motor equations in a reference frame that rotates with the rotor flux vector.

Although this method seems a viable solution, it suffers from some drawbacks, especially in high performance systems where accurate tracking is required. These drawbacks are due primarily to the fact that: 1- the motor model is highly non linear, 2- two of the state variables (rotor flux components) are usually not measurable, and 3- some parameters (rotor resistance in particular) vary significantly during operation. For these reasons, many researchers were driven to seek more complex non linear control algorithms that compensate these issues.

Rotor flux feedback was needed for these schemes, and many observers were suggested. Some researchers used Luenberger observers [1]–[3], others used the sliding mode technique [4] while others used adaptive schemes to compensate for parameter uncertainties [5], [6]. The design of the controller itself has also taken many directions. Feedback linearization [5], [7]–[10], passivity based approach [11]–[14] and sliding mode techniques [15], [16] have all been investigated and studied.

In this paper, we will develop an innovative combination of controller and observer designs. The controller is an extension of the FOC scheme designed to correct for the rotor flux steady state errors. The observer is based on the sliding mode technique, making it independent of the motor parameters. The control problem is geared toward the HEV case, and minimization of the consumed energy is also considered through the way that the flux reference curve is generated.

II. MOTOR MODEL

The motor model is described by the following set of equations [17], [18]

$$\begin{aligned} \dot{i}_d &= \left(-\frac{R_s}{\sigma} - \alpha L_m \beta\right) i_d + \omega_e i_q \\ &+ (\alpha \beta) \psi_d + \beta \omega_r \psi_q + \frac{1}{\sigma} u_d \end{aligned} \quad (1a)$$

$$\begin{aligned} \dot{i}_q &= \left(-\frac{R_s}{\sigma} - \alpha L_m \beta\right) i_q - \omega_e i_d \\ &+ (\alpha \beta) \psi_q - \beta \omega_r \psi_d + \frac{1}{\sigma} u_q \end{aligned} \quad (1b)$$

$$\dot{\psi}_d = -\alpha \psi_d + (\omega_e - \omega_r) \psi_q + \alpha L_m i_d \quad (1c)$$

$$\dot{\psi}_q = -\alpha \psi_q - (\omega_e - \omega_r) \psi_d + \alpha L_m i_q \quad (1d)$$

$$\dot{\omega}_r = \frac{P}{2J} (k_T (\psi_d i_q - \psi_q i_d) - T_l) \quad (1e)$$

where

- i_d, i_q, u_d, u_q are the stator current vector and voltage vector components in the dq rotating reference frame,
- ψ_d, ψ_q are the rotor flux vector dq components,
- ω_e is the rotating reference frame velocity,
- ω_r is the electrical rotor speed,
- T_l is the load torque and J the rotor shaft inertia,
- $\alpha, \beta, \sigma, k_T$ are given by

$$\alpha = \frac{R_r}{L_r}, \beta = \frac{L_m}{L_r \sigma}, \sigma = \frac{L_s L_r - L_m^2}{L_r}, k_T = \frac{3 P L_m}{2 L_r}$$

R_s and R_r are the stator and rotor resistances. L_s, L_r and L_m are the stator, rotor and mutual inductances respectively and P is the number of poles.

In this model, it is important to emphasize that the model inputs are u_d, u_q and ω_e , the states are i_d, i_q, ψ_d, ψ_q and ω_r .

A reduced model is usually used in the design of an induction motor drive system. As a matter of fact, the two current components i_d and i_q can be thought of as the control inputs to (1c), (1d) and (1e). The current dynamics in (1a) and (1b) can be controlled by either using a current-fed inverter, or using high gain PI regulators in the case of a voltage-fed inverter [7], [9]. The reduced order model is then described by

$$\dot{\psi}_d = -\alpha \psi_d + (\omega_e - \omega_r) \psi_q + \alpha L_m i_d \quad (2a)$$

$$\dot{\psi}_q = -\alpha \psi_q - (\omega_e - \omega_r) \psi_d + \alpha L_m i_q \quad (2b)$$

$$\dot{\omega}_r = \frac{P}{2J} (k_T (\psi_d i_q - \psi_q i_d) - T_l) \quad (2c)$$

where the control inputs are now i_d, i_q and ω_e . The states are simply ψ_d, ψ_q and ω_r .

III. THE CONTROL PROBLEM IN THE HEV CASE

In the HEV case, the electric drive subsystem is required to provide the torque requested by the supervisory controller in an accurate and efficient fashion. Another requirement, which is commonly added when controlling the induction motor, is to make the rotor flux track a certain reference

ψ_{ref} . This reference is commonly set to a value that generates maximum torque and avoids magnetic saturation, and is weakened to limit stator currents and voltages as rotor speed increases. In this paper, however, the flux reference is selected to minimize the consumption of electrical energy as it is one of the primary objectives in hybrid electric vehicles. The control problem can therefore be stated as the following torque and flux tracking problems:

$$\min_{i_d, i_q, \omega_e} \|T_e(t) - T_{eref}(t)\| \quad (3a)$$

$$\min_{i_d, i_q, \omega_e} \|\psi_d(t) - \psi_{ref}(t)\| \quad (3b)$$

$$\min_{i_d, i_q, \omega_e} \|\psi_q(t)\| \quad (3c)$$

where ψ_{ref} is selected to minimize the consumption of electrical energy. $T_{eref}(t)$ is the torque command issued by the supervisory controller while $T_e(t)$ is the actual motor torque given by

$$T_e = k_T (\psi_d i_q - \psi_q i_d) \quad (4)$$

Equation (3c) reflects the constraint of field orientation commonly encountered in the literature, and which states that the rotor flux vector be oriented with the d axis of the rotating reference frame. The control problem is illustrated in Figure 2.

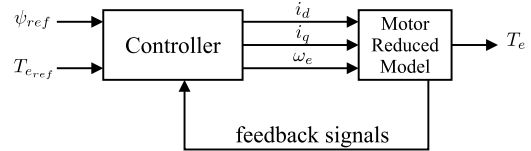


Fig. 2. The control problem.

IV. CONTROLLER DESIGN

A. Core Controller Design

The controller in Figure 2 is split in a core controller and an observer. The core controller is based on the Field Oriented Controller (FOC) scheme. The FOC solution is a simple mapping between the inputs i_d, i_q, ω_e and the reference signals $T_{eref}, \psi_{dref} = \psi_{ref}$, and $\psi_{qref} = 0$. Using (4) and solving for the control inputs in (2) when $T_e = T_{eref}$ (torque tracking), $\psi_d = \psi_{ref}$ (flux tracking), and $\psi_q = 0$ (field orientation) yields the following FOC equations:

$$i_d = \frac{\psi_{ref}}{L_m} + \frac{\dot{\psi}_{ref}}{\alpha L_m} \quad (5a)$$

$$i_q = \frac{T_{eref}}{k_T \psi_{ref}} \quad (5b)$$

$$\omega_e = \omega_r + \alpha L_m \frac{i_q}{\psi_{ref}} \quad (5c)$$

From its structure, the FOC controller resembles an open loop controller since the errors between the outputs and their references are not used. Because of its inherent open loop

design, the FOC controller has lower performance in the presence of parameter uncertainties. Since input i_d controls the flux magnitude and input ω_e controls its orientation (ω_e is the speed of the dq rotating reference frame), the FOC controller can be improved by adding two PI regulators on the error signals $\psi_d - \psi_{ref}$ and $\psi_q - 0$ as follow

$$i_d = \frac{\psi_{ref}}{L_m} + \frac{\dot{\psi}_{ref}}{\hat{\alpha}L_m} - K_{pd}(\psi_d - \psi_{ref}) - K_{id} \int (\psi_d - \psi_{ref}) dt \quad (6a)$$

$$i_q = \frac{T_{eref}}{k_T \psi_{ref}} \quad (6b)$$

$$\omega_e = \omega_r + \hat{\alpha}L_m \frac{i_q}{\psi_{ref}} + K_{pq}\psi_q + K_{iq} \int \psi_q dt \quad (6c)$$

The parameter $\hat{\alpha}$ reflects an offline estimation of the rotor resistance ($\alpha = R_r/L_r$) since the real value changes during operation and therefore is not known. Our controller is different from the commonly used PI-based FOC controller which applies the PI regulators to (6a) and (6b) only. Here the second PI regulator is used to generate the control input ω_e instead of i_q because it better reflects the control of ψ_q . This new controller relies on knowing the values of ψ_d and ψ_q . Because in most cases flux measurement is not available, the construction of an observer is needed. This is discussed in the next section.

B. Observer Design

Due to the fact that our controller presents less sensitivity to rotor resistance variations, primarily because of the two PI regulators, the design of the observer must be robust to rotor resistance uncertainty. The observer described here is based on the sliding mode technique described in [4], [19], [20]. The system equations in (1) can be put in a matrix form as

$$\begin{bmatrix} \dot{\mathbf{i}} \\ \dot{\boldsymbol{\psi}} \end{bmatrix} = \underbrace{\begin{bmatrix} \alpha\beta I + \beta\omega_r J & -\left(\frac{R_s}{\sigma} + \alpha L_m \beta\right) I + \omega_e J \\ -\alpha I + (\omega_e - \omega_r) J & \alpha L_m I \end{bmatrix}}_A \begin{bmatrix} \mathbf{i} \\ \boldsymbol{\psi} \end{bmatrix} + \underbrace{\begin{bmatrix} \mathbf{0} \\ \frac{1}{\sigma} I \end{bmatrix}}_B \mathbf{u} \quad (7a)$$

$$\mathbf{i} = \underbrace{\begin{bmatrix} I & \mathbf{0} \end{bmatrix}}_C \begin{bmatrix} \mathbf{i} \\ \boldsymbol{\psi} \end{bmatrix} \quad (7b)$$

with the measured current vector \mathbf{i} as the output. I is the 2×2 identity matrix and J is defined by $J^2 = -I$.

The observer structure, as described in [4], [19], [20], is

$$\begin{bmatrix} \dot{\hat{\mathbf{i}}} \\ \dot{\hat{\boldsymbol{\psi}}} \end{bmatrix} = A \begin{bmatrix} \hat{\mathbf{i}} \\ \hat{\boldsymbol{\psi}} \end{bmatrix} + B\mathbf{u} + \begin{bmatrix} \mathbf{v}_i \\ \mathbf{v}_\psi \end{bmatrix} \quad (8)$$

where \mathbf{i} , \mathbf{u} , ω_r are available from measurements, and ω_e is a controller internal variable. α is replaced by $\hat{\alpha}$ in A since

the true rotor resistance is not known inside the observer. The additional terms \mathbf{v}_i and \mathbf{v}_ψ are designed as

$$\mathbf{v}_i = L_i \text{sign}(\mathbf{i} - \hat{\mathbf{i}}) \quad (9a)$$

$$\mathbf{v}_{x_2} = L_\psi \text{sign}(A_{12}^{-1}(\mathbf{v}_i)_{eq}) \quad (9b)$$

where $L_i = \begin{bmatrix} l_1 & 0 \\ 0 & l_2 \end{bmatrix}$, $L_\psi = \begin{bmatrix} l_3 & 0 \\ 0 & l_4 \end{bmatrix}$ are 2×2 gain matrices and

$$A_{12} = \alpha\beta I + \beta\omega_r J \quad (10)$$

$(\mathbf{v}_i)_{eq}$ is obtained from a high-low pass filter described by

$$\tau_i(\dot{\mathbf{v}}_i)_{eq} + (\mathbf{v}_i)_{eq} = \mathbf{v}_i \quad (11)$$

where $\tau_i = \begin{pmatrix} \tau_1 & 0 \\ 0 & \tau_2 \end{pmatrix}$ contains the filter time constants.

V. FLUX REFERENCE SELECTION

The closed loop system, with its PI-based FOC controller and sliding mode observer, is shown in Figure 3. ψ_{ref} is the rotor flux reference signal yet to be defined. This section shows how it is derived in order to minimize the consumption of electrical energy instead of maximizing the motor torque as is usually done in induction motor drive systems. The flux reference derived from maximizing the torque, and referred henceforth in this paper as the standard flux reference, is based on keeping it constant up to a certain rotor base speed and decreasing it in an inverse proportion to the speed above this base speed. This weakening region is needed in order to limit the back EMF [21]. The standard flux reference does not minimize the electrical losses, and therefore is not suited for hybrid electric vehicles. In fact, for small torque requests one need not keep the flux at a higher value when a smaller value might be used to provide the same torque. Higher values of the flux consume more current and, hence, require more energy. An optimal flux reference based on minimizing power consumption was given in [22], [23]. However, the flux reference there was expressed in term of rotor speed reference input since the authors considered a speed tracking problem rather than a torque tracking problem.

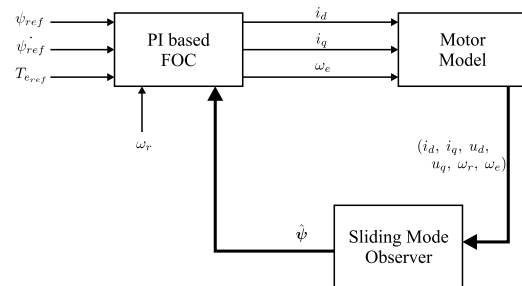


Fig. 3. Closed loop system.

To find a new ψ_{ref} selection that minimizes power losses, we first derive the expression of the losses and then

minimize it. We assume steady state analysis here. The input power is equal to

$$P_{in} = \underbrace{\frac{3}{2} [R_s (i_d^2 + i_q^2)]}_{\text{Stator Resistance Losses}} + \underbrace{\frac{3}{2} \frac{L_m}{L_r} \omega_e \psi i_q}_{\text{Air Gap Power}} \quad (12)$$

and the output power is

$$P_{out} = \omega_m T_e = \frac{3}{2} \frac{L_m}{L_r} \omega_r \psi i_q \quad (13)$$

where ψ is the rotor flux magnitude and ω_m is the rotor shaft velocity. Subtracting (13) from (12) yields the power losses expression

$$P_{Loss} = \underbrace{\frac{3}{2} R_s (i_d^2 + i_q^2)}_{\text{Stator losses}} + \underbrace{\frac{3}{2} \frac{L_m}{L_r} (\omega_e - \omega_r) \psi i_q}_{\text{Rotor losses}} \quad (14)$$

Substituting the steady state values of i_d , i_q and $\omega_e - \omega_r$, derived from (2), in (14) yields the new expression of the power losses

$$P_{Loss} = \frac{3}{2} \left[R_s (\psi/L_m)^2 + (R_s + (L_m/L_r)^2 R_r) \left(\frac{T_e}{k_T \psi} \right)^2 \right] \quad (15)$$

Minimizing (15) gives the new selection of the flux reference

$$\psi_{ref} = k_{opt} \sqrt{|T_{eref}|} \quad (16)$$

where

$$k_{opt} = \sqrt{\frac{L_m}{k_T} \sqrt{1 + \left(\frac{L_m}{L_r} \right)^2 \frac{R_r}{R_s}}} \quad (17)$$

Equation (16) states that at low torque levels, the flux level should be also low in order to consume less energy. However, equation (6b) presents a singularity if the torque request T_{eref} is zero. Moreover, the analysis carried out here does not consider the constraints on stator currents and voltages. Indeed, the stator currents and voltages cannot exceed their maximum physical values which is described by the weakening region in the standard flux reference selection. To solve the singularity problem, we can set a non zero minimum value for the flux reference signal, whereas to solve the current and voltage constraints, we can take the standard flux reference shape as the maximum value. The new optimum flux reference signal is then described by

$$\psi_{ref} = \begin{cases} \psi_{opt} = k_{opt} \sqrt{|T_{eref}|} & \text{if } \psi_{min} < \psi_{opt} \leq \psi_{max}, \\ \psi_{min} & \text{if } \psi_{opt} \leq \psi_{min}, \\ \psi_{max} & \text{if } \psi_{opt} \geq \psi_{max}. \end{cases} \quad (18)$$

where ψ_{min} is a minimum value to avoid the division by zero and

$$\psi_{max} = \begin{cases} \psi_0 & \text{if } |\omega_r| \leq \omega_b \\ \frac{\omega_b}{|\omega_r|} \psi_0 & \text{if } |\omega_r| > \omega_b \end{cases} \quad (19)$$

is the standard flux reference shape formed by a constant flux ψ_0 (maximum flux without saturation) up to a base speed ω_b and weakening beyond this base speed.

VI. SIMULATIONS

The torque reference curve that is used in the simulations is shown in Figure 4. It represents typical acceleration, constant speed, and deceleration behaviors in a hybrid electric vehicle. Negative torque request is also selected to simulate the regenerative mode. Load torque is modeled by considering the aerodynamic, rolling resistance and road grade forces. Its expression is given by

$$T_l = \frac{R_{tire}}{R_f} \left[\underbrace{\frac{1}{2} \rho_{air} C_d A_f v^2}_{\text{aerodynamic}} + \underbrace{M g C_r \cos \alpha_g}_{\text{rolling resistance}} + \underbrace{M g \sin \alpha_g}_{\text{grade}} \right] \quad (20)$$

where ρ_{air} is the air density, C_d is the aerodynamic drag coefficient, A_f is the frontal surface area of the vehicle, M is the mass of the vehicle, α_g is the grade angle, C_r is the rolling resistance coefficient, and v is the vehicle speed related to the motor shaft velocity by $v = (R_{tire}/R_f) \omega_m$, where R_{tire} is the radius of the tires and R_f is the total ratio between the motor shaft and the differential axle of the vehicle.

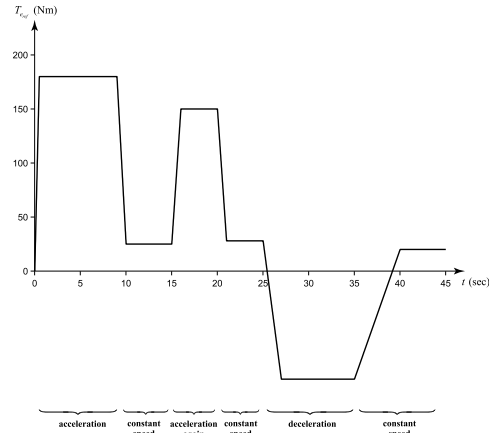


Fig. 4. The Torque reference curve.

The numerical values of the parameters that are used in the simulations are given by

$$\begin{aligned} R_s &= 0.014 \Omega, R_r = 0.009 \Omega, \\ L_{ls} &= 75 \mu\text{H}, L_{lr} = 105 \mu\text{H}, L_m = 2.2 \text{ mH}, \\ L_s &= L_{ls} + L_m, L_r = L_{lr} + L_m, \\ P &= 4, J_{mot} = 0.045 \text{ Kg}\cdot\text{m}^2, J = J_{mot} + M \frac{R_{tire}^2}{R_f}, \\ \rho_{air} &= 1.29, C_d = 0.446, A_f = 3.169 \text{ m}^2, R_f = 8.32, \\ C_r &= 0.015, R_{tire} = 0.3683 \text{ m}, M = 3000 \text{ kg}, \\ \psi_0 &= 0.47 \text{ Wb}, \omega_b = 5400 \text{ rpm}. \end{aligned}$$

In Figure 5, we compare power losses and efficiency results using the new optimal flux reference with the results using the standard flux reference. The simulation was carried out using the non regulated FOC controller in (5). The power losses plot show that the system consumes less

energy with the new optimal flux reference. For the 45 seconds of simulation, energy losses using the standard flux reference were 51.5 kJ while they were 33.5 kJ with the new flux reference. This 35% reduction in energy losses is primarily due to reducing the flux reference during the periods of low torque requests. Figure 5b shows significant improvement in power efficiency during steady state periods.

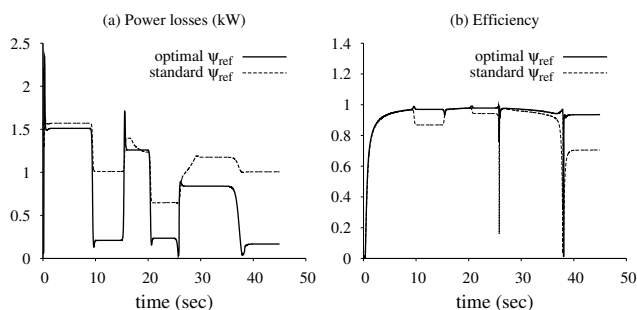


Fig. 5. Power losses (a) and efficiency (b) with optimal (solid) and standard (dashed) ψ_{ref} .

Figures 6 - 13 show the simulation results of the closed loop system of Figure 3. The controller parameters used in the simulation are: $K_{pd} = 0$, $K_{id} = 0.1$, $K_{pq} = 0.1$, $K_{qi} = 200$, $l_1 = 7$, $l_2 = 10$, $l_3 = 2$, $l_4 = 1$ and $\tau_1 = \tau_2 = 0.004$.

In the first set, i.e. Figures 6 - 9, we used the true value of the rotor resistance inside the controller, whereas in the second set, i.e. Figures 10 - 13, we simulated the extreme case of rotor resistance uncertainty by using half the value of the rotor resistance ($\hat{R}_r = 0.5R_r$) inside the controller.

Figures 6 and 10 are plots of the motor torque (solid line), the reference torque (dotted line) and the load torque (dashed line) for both cases. Good torque tracking is achieved even with the rotor resistance uncertainty. Figures 8, 9, 12 and 13 represent the d and q components of the rotor flux for both cases. A small steady state error can be noticed on the observed fluxes for the uncertain case. However, flux and torque tracking are still achieved at an acceptable level as shown in Figures 10, 12 and 13. Figures 7 and 11 represents the motor and vehicle speeds and show clearly the different phases of acceleration, constant speed and deceleration. It is worth notice also that stator currents and voltages never reached their maximum values during simulation due to the upper limit imposed on the flux reference in (18).

VII. CONCLUSION

In this paper, a new flux reference has been derived in order to minimize the use of electrical energy, which is a major factor in designing motor drive systems for hybrid electric vehicles. The flux reference is shown to be proportional to the square root of the torque reference input. An innovative robust controller for the induction motor has been proposed. The new controller, which is a combination of a new PI-based extension of the FOC

controller and a sliding mode observer, showed good closed loop performance (good flux and torque tracking) even in the presence of rotor resistance uncertainty.

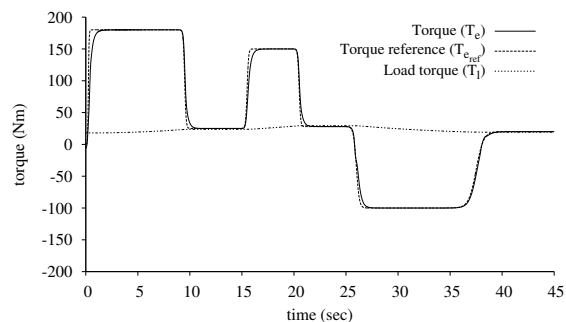


Fig. 6. Motor torque - (known R_r).

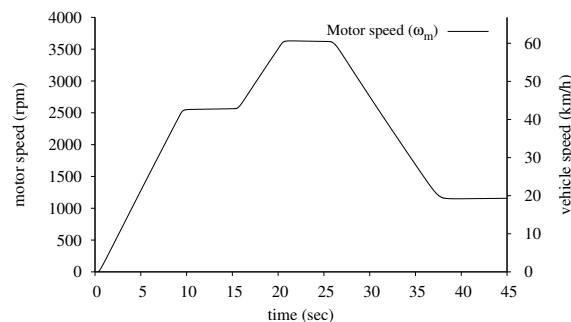


Fig. 7. Motor/Vehicle speed - (known R_r).

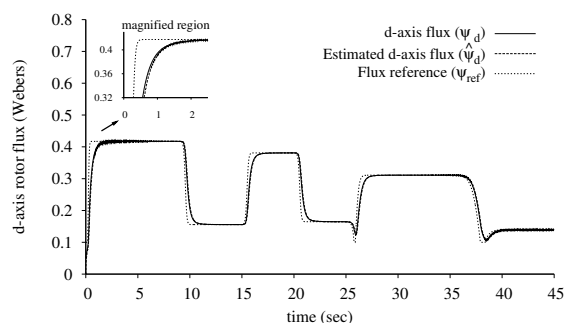


Fig. 8. Rotor flux d component - (known R_r).

REFERENCES

- [1] G. Verghese, "Observers for flux estimation in induction machines," *IEEE Trans. on Industrial Electronics*, vol. 35, no. 1, Feb. 1988.
- [2] A. Medvedev, "On robust stability of two flux observers for induction machines," in *Proc. of the 1999 IEEE International Conference on Control Applications*, Kohala Coast-Island, Hawaii, Aug. 1999, pp. 962-967.
- [3] —, "A guaranteed performance flux observer for induction machines," in *Proc. of the 36th Conference on Decision and Control*, San Diego, CA, Dec. 1997, pp. 229-232.
- [4] S. V. Drakunov and V. Utkin, "Sliding mode observers. tutorial," in *Proc. of the 34th Conference on Decision and Control*, New Orleans, LA, Dec. 1995, pp. 3376-3378.

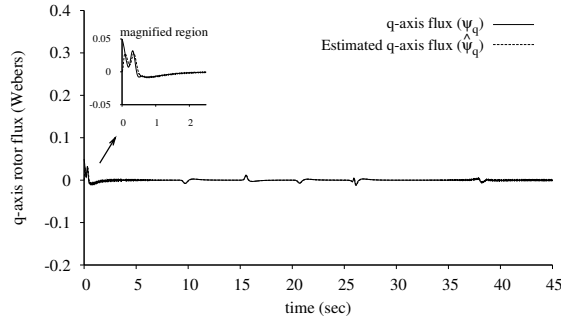


Fig. 9. Rotor flux q component - (known R_r).

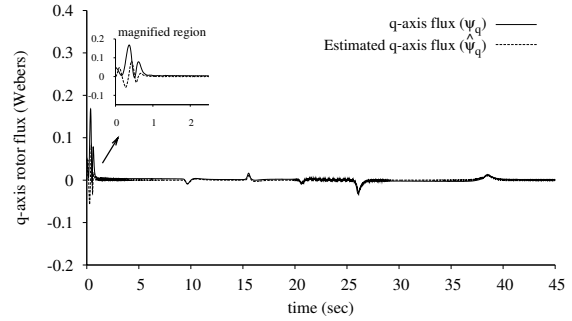


Fig. 13. Rotor flux q component - (underestimated R_r).

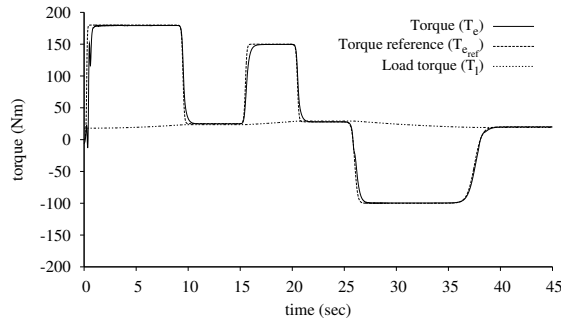


Fig. 10. Motor torque - (underestimated R_r).

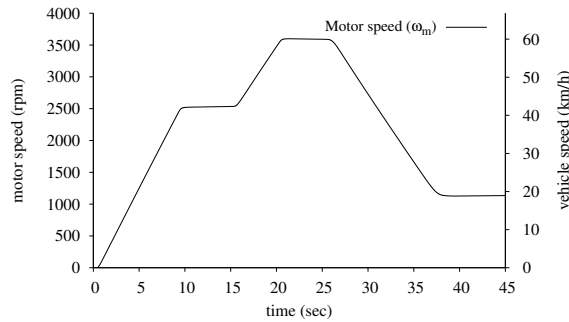


Fig. 11. Motor/Vehicle speed - (underestimated R_r).

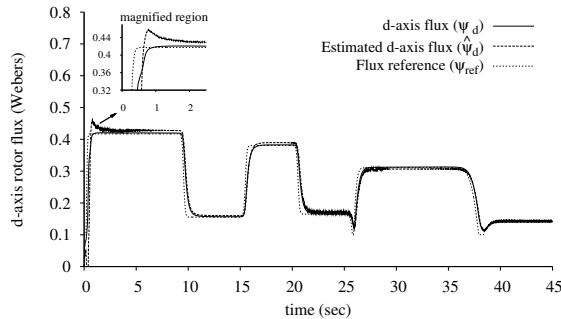


Fig. 12. Rotor flux d component - (underestimated R_r).

[5] R. Marino, S. Peresada, and P. Tomei, "Adaptive observer-based control of induction motors with unknown rotor resistance," *International Journal of Adaptive Control and Signal Processing*, vol. Vol. 10, pp. 345–363, 1996.

[6] R. Marrino, S. Peresada, and P. Tomei, "On-line stator and rotor

resistance estimation for induction motors," *IEEE Trans. on Control Systems Technology*, vol. Vol. 8, no. No. 3, May 2000.

[7] M. Bodson, J. Chiasson, and R. Novotnak, "High performance induction motor control via input-output linearization," *IEEE Control Systems magazine*, vol. Vol. 14, no. No.4, Aug. 1994.

[8] J. Chiasson, "A new approach to dynamic feedback linearization control of an induction motor," *IEEE Trans. on Automatic Control*, vol. Vol. 43, no. No. 3, May 1998.

[9] R. Marrino, S. Peresada, and P. Tomei, "Output feedback control of current-fed induction motors with unknown rotor resistance," *IEEE Trans. on Control System Technology*, vol. Vol. 4, no. No. 4, May 1996.

[10] R. T. Novotnak, "Nonlinear control of an induction motor by input/output linearization: Theory and experiment," Ph.D. dissertation, University of Pittsburgh, Pittsburgh, PA, 1995.

[11] G. Chang, G. Espinosa, and R. O. E. Mendes, "Tuning rules for the pi gains of field-oriented controllers of induction motors," *IEEE Trans. on Industrial Electronics*, vol. Vol. 47, no. No. 3, June 2000.

[12] G. Espinosa, R. Ortega, and P. Nickalsson, "Torque and flux tracking of induction motors," *International Journal of Robust and Nonlinear Control*, vol. Vol. 7, no. No., pp. 1–9, 1997.

[13] K. Kim, R. Ortega, A. Charara, and J. Vilain, "Theoretical and experimental comparison of two nonlinear controllers for current-fed induction motors," *IEEE Trans. on Control Systems Technology*, vol. Vol. 5, no. No. 3, May 1997.

[14] R. Ortega and G. Espinosa, "Torque regulation of induction motors," *Automatica*, vol. Vol. 29, no. No. 3, pp. 621–663, 1993.

[15] S. Drakunov, V. Utkin, S. Zarei, and J. Miller, "Sliding mode observers for automotive applications," in *Proc. of the 1996 IEEE International Conference on Control Applications*, Dearborn, MI, Sept. 1996, pp. 344–346.

[16] V. I. Utkin, "Sliding mode control design principles and applications to electric drives," *IEEE Trans. on Industrial Electronics*, vol. Vol. 40, no. No. 1, Feb. 1993.

[17] A. M. Trzynadlowski, *The Field Orientation Principle in Control of Induction Motors*. Boston: Kluwer Academic Publishers, 1994.

[18] P. Vas, *Vector Control of AC Machines*. NY: Oxford University Press, 1990.

[19] S. V. Drakunov, "Sliding mode observers based on equivalent control method," in *Proc. of the 31st Conference on Decision and Control*, Tuscon, AZ, Dec. 1992, pp. 2368–2369.

[20] V. Utkin, J. Guldner, and J. Shi, *Sliding Mode Control in Electromechanical Systems*. Philadelphia: Taylor & Francis, 1999.

[21] M. Bodson, J. Chiasson, and R. Novotnak, "A systematic approach to selecting flux references for torque maximization in induction motors," *IEEE Trans. on Control Systems Technology*, vol. Vol. 3, no. No. 4, Nov. 1995.

[22] D. Kim, I. Ha, and M. Ko, "Control of induction motors via feedback linearization with input-output decoupling," *International Journal of Control*, vol. 51, no. 4, pp. 863–883, 1990.

[23] G. Kim, I. Ha, and M. Ko, "Control of induction motors for both high dynamic performance and high-power efficiency," *IEEE Trans. on Industrial Electronics*, vol. 39, no. 4, pp. 323–333, August 1992.